Arabian Journal of Chemistry (2014) 7, 27–36

King Saud University

Arabian Journal of Chemistry

www.ksu.edu.sa
www.sciencedirect.com

SPECIAL ISSUE: ENVIRONMENTAL CHEMISTRY

Development, characterization and evaluation of iron-coated honeycomb briquette cinders for the removal of As(V) from aqueous solutions

Tiantian Sheng, Shams Ali Baig, Yunjun Hu, Xiaoqin Xue, Xinhua Xu *

College of Environmental and Resource Sciences, Department of Environmental Engineering, Zhejiang University, Hangzhou 310058, People's Republic of China

Received 12 March 2013; accepted 31 May 2013
Available online 2 July 2013

KEYWORDS

Adsorption;
Characterization;
Desorption;
Granulation;
Separations;
Solutions

Abstract The adsorptive removal of As(V) from aqueous solutions using iron-coated honeycomb briquette cinder (Fe-HBC) is presented. Low cost mechanical granulation process was integrated with surface amendment technology to prepare iron-oxide modified granular adsorbent for clean water production. Detailed characterizations were performed using FTIR, XRD, EDS and SEM techniques. Operating parameters including initial As(V) concentration, pH, contact time, adsorbent dose, iron leaching and the effects of competing ions on As(V) removal were evaluated. Results demonstrated that high amount of arsenate (961.5 μg g^{-1}) was adsorbed at pH 7.5 in 14 h contact time. Langmuir, Freundlich and Temkin isotherm models were used to analyze the adsorption data, whereas Langmuir model was found to best represent the data with a correlation co-efficient (R^2 = 0.999). Thus, As(V) sorption on Fe-HBC surface suggested monolayer adsorption and indicated surface homogeneity. Moreover, the dimensionless parameter (R_L) value calculated to be about 0.118 that reiterated the process is favorable and spontaneous. The influences of competing ions on As(V) removal decreased in the following order: $PO_4^{3-} > HCO_3^- > F^- > Cl^-$. The profound inhibition effects of PO_4^{3-} revealed a high affinity toward iron(oxy) hydroxide. Life-cycle assessment confirmed that spent HBC is non-hazardous and can be used as a promising sorbent for arsenic removal.

1. Introduction

Arsenic (As) is naturally distributed in different environmental components and its elevated concentration in drinking water threatens to over 200 million people worldwide (Mandal and Suzuki, 2002; Mohan and Pittman, 2007). Arsenic above World Health Organization (WHO) permissible limit is detected in both developing and developed countries; including USA, China, Argentina, Mexico and Pakistan (Malik et al.,

* Corresponding author. Tel./fax: +86 571 88982031.
E-mail address: xuxinhua@zju.edu.cn (X. Xu).

Peer review under responsibility of King Saud University.

Production and hosting by Elsevier

1878-5352 © 2013 Production and hosting by Elsevier B.V. on behalf of King Saud University.
http://dx.doi.org/10.1016/j.arabjc.2013.05.032

2009). According to the recent estimates; arsenic poisoning in Bangladesh and West Bengal (India) has turned far more disastrous. Many drinking water wells contain over 200 ppb dissolved arsenic, while the recommended value is 10 ppb. However, the presence of elevated level of dissolved arsenic in water does not harm its color, taste and odor (Sarkar et al., 2005; WHO, 2011).

Generally, many biogeochemical processes and anthropogenic actions release arsenic and its mobilization to groundwater is facilitated by natural circumstances. Arsenic directly or indirectly reaches to water bodies from the combustion of fossil fuels and arsenic additives in herbicides, pesticides, livestock feeder (Genc-Fuhrman et al., 2004a; Mohan et al., 2007). Elevated arsenic concentration in drinking water causes cancer to human internal organs and can also induce cardiovascular effects. Hence, arsenic has been classified as a Group 1 carcinogenic element based on WHO epidemiological verification (USEPA, 2000; WHO, 2011). Because of the adverse health consequences of high arsenic exposure, various countries worldwide amend their water quality guidelines and reduce its permissible limits to 10 ppb from 50 ppb in drinking water supply (WHO, 2011).

In water environment, inorganic arsenic predominantly exits as arsenite (As(III)) and arsenate (As(V)). In principle, arsenite species (AsO_3^{3-}, $As(OH)^3$, $As(OH)^{4-}$ and AsO_2OH^{2-}) are primarily available in reducing environments, whereas, H_3AsO_4, $H_2AsO_4^-$, $HAsO_4^{2-}$ and AsO_4^{3-} species of arsenate are usually stable in oxidizing conditions (Bodek et al., 1998; Genc-Fuhrman et al., 2004b). Therefore, arsenate dominant availability in drinking water sources attracts researchers' attentions to develop some remediation measures in recent years. Moreover, arsenite; if present can be readily oxidized to arsenate from different conventional methods for the optimal removal of arsenic from surface water sources (Genc-Fuhrman et al., 2004b, 2005; Mohan et al., 2007).

Among various available arsenic removal technologies; adsorption is considered to be feasible because of easy operation, high adsorptive efficiency, cost-effectiveness and durability (Jing et al., 2012; Repo et al., 2012; Baig et al., 2013). Adsorption on iron bearing adsorbents has been successfully tested to remove arsenic from water (Genc-Fuhrman et al., 2004a; Gu et al., 2005; Hristovski et al., 2009). Moreover, extensive studies have been carried out on various aspects of cost-effective adsorbents including iron fabrication, surface characterizations and arsenic removal performance in recent years (Kundu and Gupta, 2006, 2007a; Dong et al., 2009; Mathieu et al., 2010; Barakat and Shah, 2013; Chen et al., 2012; Maji et al., 2012; Francesca et al., 2013). Honeycomb briquette cinders (HBC) were locally generated during the combustion of coal-based honeycomb briquettes and mostly used in civil applications. Recently, Yue et al. (2011) explored its scientific applicability to eliminate COD_{cr} and phosphate from landfill leachate. Realizing HBC promising surface morphology, granular structure and local-based massive generation, there was an urgent need to utilize and necessarily modify this material for adsorptive removal of arsenic from water. In this study, we investigate its possible application to remove arsenic from aqueous medium.

The aim of this study was to evaluate the adsorptive efficiency of iron-coated adsorbent (Fe-HBC) for removing As(V) in aqueous solutions. Various operating parameters including initial As(V) concentration; pH, contact time, adsorbent dose and the effects of competing ions on As(V) removal were investigated. FTIR, XRD, EDS and SEM were also applied to characterize the adsorbent. Furthermore, the obtained data were then tested using various equilibrium isotherm and kinetic models to indentify/discuss the possible adsorption mechanisms.

2. Materials and methods

2.1. Reagents

All the reagents used in this study were of analytical grade and utilized without any further purification. Arsenate stock solution (1000 mg L^{-1}) was prepared by dissolving 0.566 g of sodium arsenate ($Na_3AsO_4{\cdot}12H_2O$) in de-ionized (DI) arsenic free water into a 100 mL volumetric flask. Desired concentration of As(V) bearing working solution was freshly prepared by diluting the stock solution in DI water prior to the experiments. Hydrochloric acid and NaOH were used to adjust the solution pH as required. Chemicals; $FeSO_4{\cdot}7H_2O$, ascorbic acid, NaOH, and HCl were obtained from Sinopharm Group Chemical Reagent Co., Ltd., China. Thiourea and KBH_4 were obtained from Aladdin Chemistry Co., Ltd., Shanghai, China. In order to prepare thiourea, KBH_4, ascorbic acid, NaOH, and HCl solutions approximate amounts of the respective compounds were dissolved in DI water.

2.2. Development of adsorbent

Fig. 1 presents the adsorbent granulation and surface coating processes. The brownish HBC wastes were obtained from a local restaurant near Zhejiang University at Hangzhou city of China. In order to make granular adsorbent the HBC wastes were crushed with a hammer and washed with tap water to remove organic constituents. The granular materials were then oven dried at 50 °C for 24 h. The dried HBC were then sieved and washed with DI water for three times. In this study, the sieved HBC granules of 0.5 mm size were purposively used to coat with Fe(II) and subsequent batch adsorption experiments.

In order to develop iron-coated HBC adsorbent (Fe-HBC), 100 g of 0.5 mm size HBC was added to 700 mL of 0.7 M aqueous $FeSO_4{\cdot}7H_2O$ solution and mechanically stirred in an ultrasonic cleanser bath for 1 h (Roberts et al., 2004; Mathieu et al., 2010). All the preparation steps were carried out at room temperature 23 ± 2 °C. Subsequently, 100 mL of 0.1 M

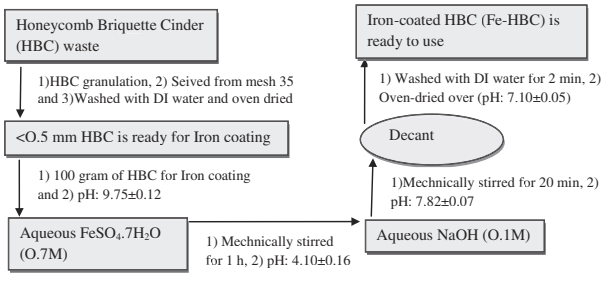

Figure 1 Schematic flow diagram presents the adsorbent granulation and surface coating processes.

NaOH aqueous solution was added and agitated for 20 min. After settling, the mixture is decanted and evenly distributed in a big dish and oven-dried at 50 °C for 24 h. In the successive day, the Fe-HBC adsorbent is congregated, examined and stored for batch adsorption experiments (Fig. 1).

2.3. Adsorption experiments

Batch adsorption experiments were performed to obtain the equilibrium data, using 250 mL glass conical flasks containing synthetic arsenic solutions kept at room temperature (23 ± 2 °C). The conical flasks were mechanically shaken at 150 rpm in a rotary shaker (SUKUN, SKY-110WX, Shangai, China) for 14 h (840 min). After the required reaction time the filtrates were then taken out using syringes and filtered through a 0.45 μm filter membrane, and the supernatant was subsequently analyzed for arsenate determination. In this study, each batch experiment was performed in triplicate and mean values were presented.

To study the effects of adsorbent dose, experiments were performed by varying the dose from 0.01 to 0.05 g in 150 mL solution with 100 μg L^{-1} initial As(V) concentration at 7.5 pH and 14 h contact time. Meanwhile, water samples for As(V) analysis were taken at preset time intervals. Afterward, adsorbent dose: 0.04 g in 150 mL solution was decided the set amount for batch arsenate adsorption and subsequently used in the remaining batch experiments. The effects of solution pH on arsenic adsorption by Fe-HBC were performed by adjusting the solution initial pH from 2 to 12 using 1 M of HCl and NaOH. Therefore, 0.04 g of Fe-HBC was added into the flasks and agitated till equilibrium time. In order to study the adsorption isotherm and the effects of initial As(V) concentration; experiments with different initial As(V) concentrations (100–500 μg L^{-1}) and adsorbent dose (0.04 g) at fixed contact time (14 h) were performed. Moreover, effects of competing ions (Cl^-, F^-, HCO_3^- and PO_4^{3-}) on As(V) removal were investigated by varying the solution concentration ranges (0–10 mM). Leaching of total iron from Fe-HBC into the solution was also tested at wide solution pH values (2–12).

2.4. Analytical methods

All the apparatuses used in the current experiment were first immersed in nitric acid solution for 24 h; washed with tap followed by DI water and then dried overnight in an oven. A digital pH meter (Mettler Toledo SG2, Shangai, China) was used to adjust the solutions pH. To measure the arsenate concentration, atomic fluorescence spectrometer (AFS-230E, Beijing China) was used (Li et al., 2010). For this purpose, a mixture of 5% L-ascorbic acid and 5% thiourea was employed as a reducing agent. Spectrophotometer (Spectrumlab 23A, Leng Guang Tech. China) was used to quantify total iron at 510 nm wave lengths.

Different techniques were used to characterize the adsorbent, as described in earlier studies (Xu et al., 2013; Zhu et al., 2013). Briefly, elemental analysis of raw adsorbent (HBC) and iron-coated adsorbent (Fe-HBC) before and after As(V) adsorption were measured by X-ray energy dispersive spectrometer (EDS, model: ESM-5800, GEOL, Japan). XRD analyses (X'pert PRO analytical B.V., Netherlands) of the samples were performed in 2θ scale. Fourier transform infrared spectrometer (FTIR) at 4000 and 400 cm^{-1} wave number (IR Prestige-21, Japan) was used to characterize the functional groups on raw HBC, Fe-HBC before and after As(V) adsorption. Scanning electron micrograph (SEM) (Hitachi S-3000 N, Japan) was used to analyze the morphological structures of raw HBC, Fe-HBC before and after As(V) adsorption.

3. Results and discussion

3.1. Characterization of Fe-HBC

Various techniques including FTIR, XRD, SEM and EDS analyses were carried out to characterize the adsorbent. Fig. 2 shows the FTIR spectra of raw HBC, Fe-HBC before and after As(V) adsorption, respectively. Peak at λ value of 492 cm^{-1} showed the surface characteristic of Fe–O vibration (Feng et al., 2012) which was reduced after arsenate adsorption on Fe-HBC. The band that appeared at λ value of 765 cm^{-1} was assigned to the symmetric stretching vibrations of Si(Al)–O (Fan et al., 2008). However, this band reduced after As(V) adsorption and clearly indicated surface complexations, attributed to the As-O–Fe group (Lakshmipathiraj et al., 2006; Repo et al., 2012). In the entire sample strong (s) band appeared at 1087 cm^{-1} showing C–O–C stretching mode. Moreover, a short band at 1696 cm^{-1} was assigned to alkenes (–C═C–) stretching in the carbon skeleton (Feng et al., 2012; Ntim and Mitra, 2012). The strong spectral band located at λ value of 3445 cm^{-1} in all the samples assigned to O–H deformation (Mikhaylova et al., 2006). The strong band at the same wave number before and after As(V) adsorption on Fe-HBC suggested an increase in $Fe(OH)_3$ bonds on HBC due to Fe^{3+}, formed from the oxidation of Fe^{2+} in overnight oven drying. Increase of FeOH bonds on the adsorbent's surface due to Fe^{3+} reflected a strong band in FTIR spectra (Fig. 2) (Mondal et al., 2008).

Fig. 3 (a–c) presents the results of XRD analysis. XRD results of Fe-HBC showed less surface complexities than the raw HBC and hence iron-coated adsorbent provided feasible surface adhesion property for As(V) adsorption (Fig. 3b) which is consistent with the previously reported studies (Yue et al., 2011; Chen et al., 2012). However, new smaller peaks at

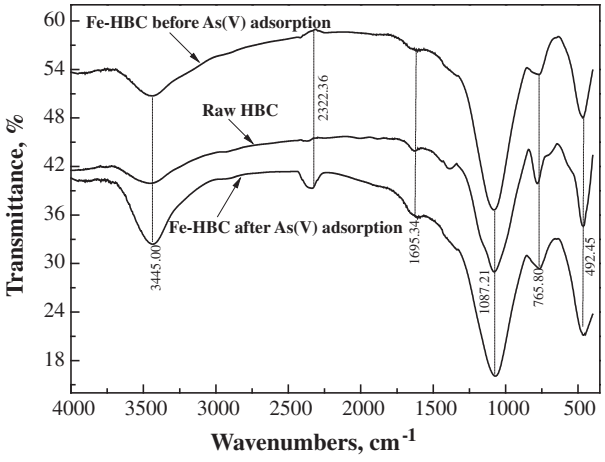

Figure 2 The results of FTIR spectra of raw HBC, Fe-HBC before and after As(V) adsorption.

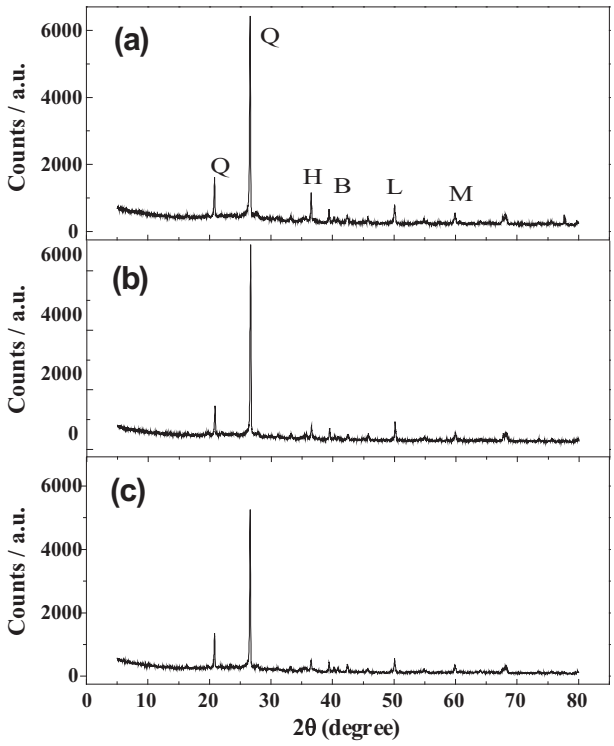

Figure 3 XRD analysis results of (a) raw HBC, (b) Fe-HBC before As(V) adsorption and (c) Fe-HBC after As(V). The adsorption's patterns show various peaks (Q: quartz(SiO_2), H: hematite(Fe_2O_3), B: boehmite(AlO(OH), L: lime(CaO) and M: magnetite(Fe_3O_4) at different 2θ scale.

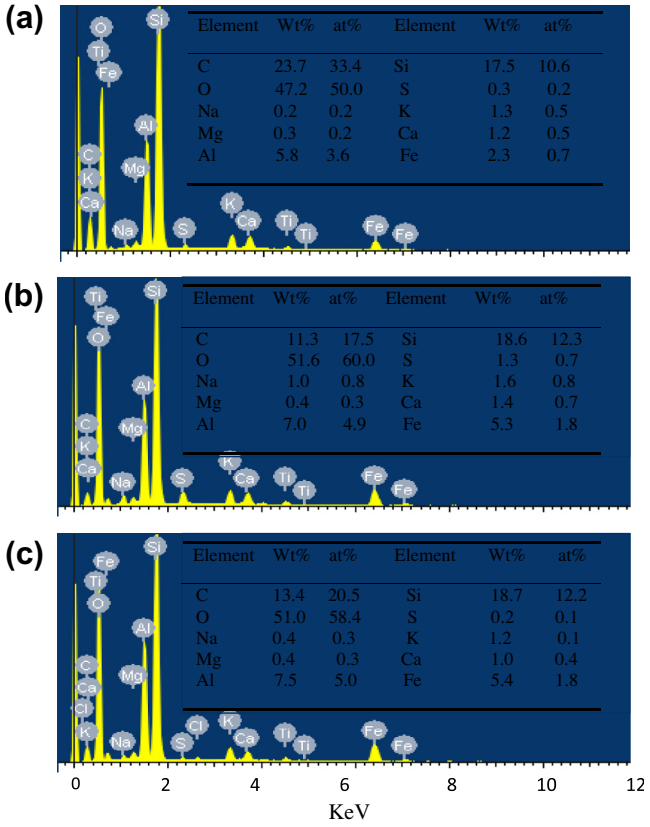

Figure 4 EDS analysis results of (a) raw HBC, (b) Fe-HBC before As(V) adsorption and (c) after As(V) adsorption.

(2θ = 60° and 68°) appeared in this study which correspond to the presence of magnetite. The appeared peaks of SiO_2, Fe_2O_3, and AlO(OH) were reduced after coating with iron and further after arsenate adsorption on its surface, as clearly shown in Fig. 3 (b and c). Fig. 4 (a–c) presents the results of EDS analysis. The increased iron values at 6.8 and 7.0 keV showed a considerable amount of coated iron on adsorbent's surface (Fig. 4b), as compared to the raw HBC (Fig. 4a). Moreover, smaller energy level appeared at about 8.0 and 8.8 keV (Fig. 4c) which might indicated Av(V) adsorption on the adsorbent surface (Li et al., 2010).

Fig. 5 shows SEM image (20 K magnification) of raw HBC (a and b), Fe-HBC before (c and d) and Fe-HBC after (e and f) As(V) adsorption, respectively. An amorphous layer of Fe^{3+} appeared on the surface of the iron-coated adsorbent formed from the oxidation of Fe^{2+} (Fig. 5c and d). Tabular crystal structures with more surface area appeared after As(V) adsorption on Fe-HBC, as shown in SEM image (Fig. 5e and f). It is evident of more As(V) adsorption on Fe-HBC and that lead to the formation of inner-sphere surface complexes through selective physical sorption. Such surface structures are believed to be more promising for emergent pollutants' remediation (Yue et al., 2011).

3.2. Adsorption experiments

3.2.1. Effect of adsorbent dose on As(V) removal

For optimizing a treatment system, it is essential to evaluate the effect of adsorbent dose and contact time required to reach equilibrium for safe drinking water production. In this study, arsenic removals at varying adsorbent dose (0.01, 0.02, 0.03, 0.04 and 0.05 g) in 150 mL solution with 100 μg L^{-1} initial arsenic concentration at different contact times were studied at pH 7.5. It was evident from Fig. 6 that As(V) removal efficiency increased with the elapse of Fe-HBC dose and the adsorption efficiency has risen from 38% to 100% at the dose of 0.01 g/150 mL to 0.05 g/150 mL, respectively. This may be caused by the availability of more exchangeable surface sites due to the more adsorbent iron-hydroxide contents (Fan et al., 2008). However, at the adsorbent dose of 0.04 g/150 mL, the removal efficiency was above 95% and hence the removal process is effective to bring the concentration of arsenic to meet WHO and US-EPA permissible limits (Genc-Fuhrman et al., 2005; Sarkar et al., 2005; WHO, 2011). Moreover, rapid adsorption of As(V) in the first 120 min can be explained by the increased number of vacant spots available for adsorption at the beginning. Thereafter, the adsorption rate decreased gradually and reached an equilibrium at about 14 h, as shown in Fig. 6. Thus, the adsorbent dose of 0.4 g/150 mL and 14 h of shaking were adopted for further study. In batch experiments with other adsorbent dosages (0.01, 0.02 and 0.03 g/150 mL) it was reiterated that with less amount of adsorbent dose: few surface sites were offered for adsorption and hence low As(V) removals were recorded at ambient temperature (Fig. 6). In this study, no adsorption differences were observed when the temperature increased to 35 °C and 45 °C, respectively (data not shown). However, low As(V)

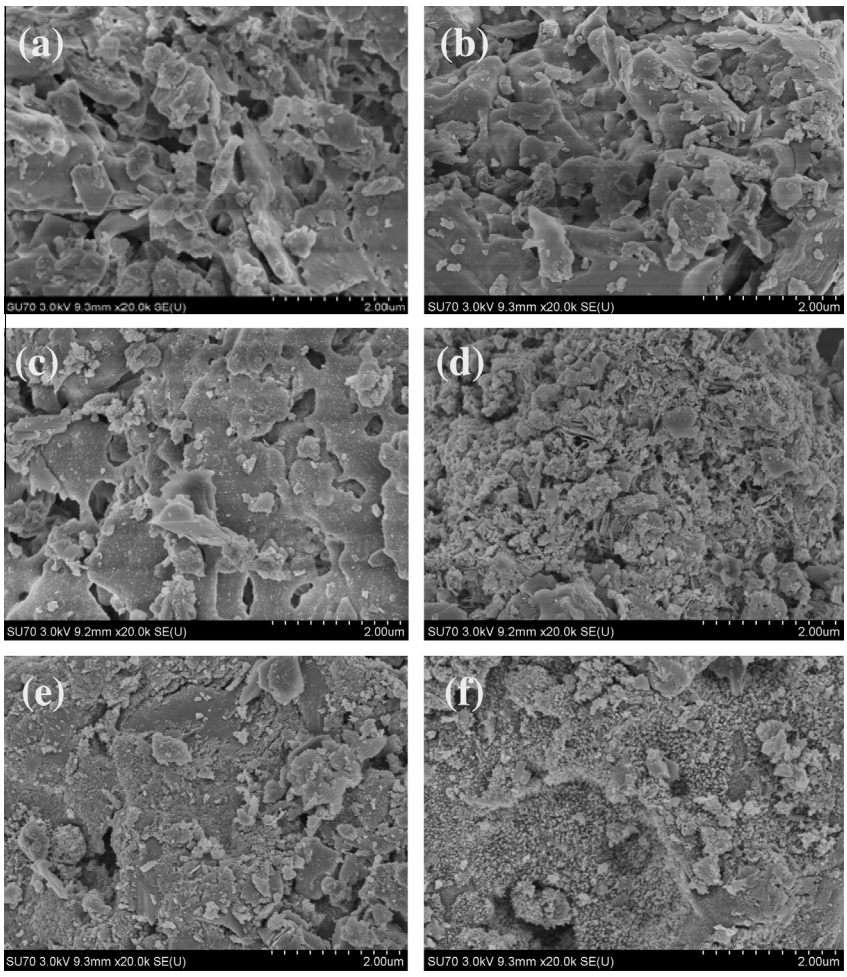

Figure 5 SEM images show (a and b) raw HBC, (c and d) Fe-HBC before As(V) adsorption and (e and f) Fe-HBC after As(V) adsorption with 20 K magnifications.

adsorption on bone char was reported when the temperature increased from 28 to 48 °C (Chen et al., 2008).

3.2.2. Effect of solution pH on As(V) removal

Several factors including adsorbent's surface charge, degree of ionization, dissociation of functional groups on the active sites and the arsenic chemical speciation are decisive for As(V) removal in aqueous solutions. In order to investigate the optimum pH for maximum arsenic removal, batch experiments were conducted using a series of arsenate solutions under the following reaction conditions: initial concentration of 100 μg L^{-1}, 0.04 g/150 mL adsorbent dose and varying initial solution pH (pH 2–12) for 14 h equilibrium time. Fig. 7 presents the result of As(V) removal at different pH values (pH 2–12) and iron leaching. It was obvious from the solution pH alteration that the removal efficiency of As(V) was around 90% at pH range of 6–9 and then decreased with further decrease or increase of solution pH. Moreover, the adsorption of arsenic was found to be optimum at pH ranges of 6–8. Different optimum pH ranges to remove As(V) using various adsorbents from the reported studies are presented in Table 1.

The results could be explained in the light of published literatures to diagnose the stability of different As(V) species at wide pH ranges: pH 0.0–2.0, 2.0–7.0, 7.0–12.0 and 12.0–14.0 reflect the presence of H_3AsO_4, $H_2AsO_4^-$, $HAsO_4^{2-}$ and AsO_4^{3-} arsenate species, respectively (Chen et al., 2008; Li et al., 2010). Therefore, the removal efficiency of different As(V) species at certain pH reflected the wide range of solution pH. At

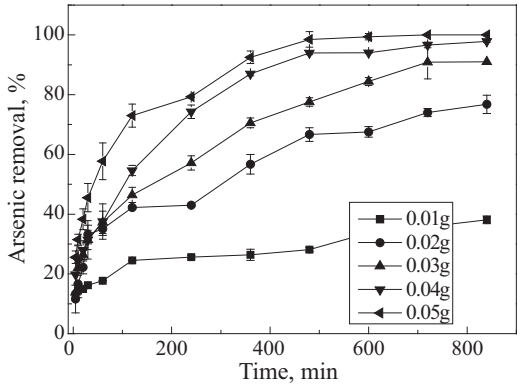

Figure 6 Effect of adsorbent dose on As(V) removal. Reaction conditions: initial As(V) concentrations = 100 ppb; volume of the reaction solution: 150 mL; contact time 14 h (840 min), solution pH: 7.5.

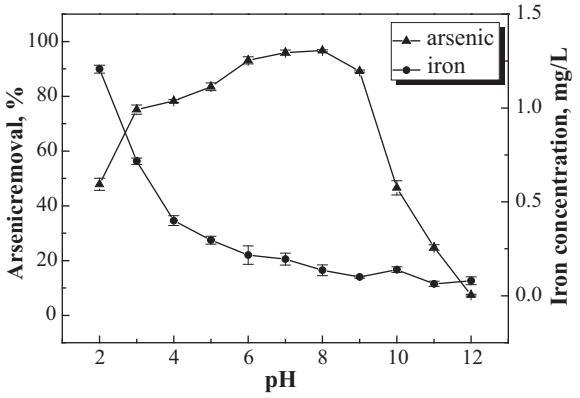

Figure 7 Effect of initial solution pH and iron concentration on As(V) removal. Reaction conditions: adsorbent dose = 0.04 g/150 mL; initial As(V) concentration = 100 ppb; equilibrium time = 14 h.

the studied pH, pentavalent arsenic mostly exists in two anionic forms ($H_2AsO_4^-$ and $HAsO_4^{2-}$), where the hydroxyl ion is replaced by the arsenate anion during ion-exchange process (Fan et al., 2008). The elevated arsenate removal efficiency of Fe-HBC at pH range 6–8 reiterated the fact that the adsorbent's surface possessed positively charged characteristic and showed a greater tendency to attract arsenate anions $HAsO_4^-$ in this range. Similarly, Repo et al. (2012) reported the same electrostatic interaction phenomenon to As(V) from aqueous solution using heat-treated lepidocrocite. Another important factor during this adsorption process was the release of iron; where a very small amount of iron dissolved into the solution when the pH was higher than 6, as shown in Fig. 7. While a decrease in removal efficiency above pH 8 can be related to the competitions for the active sites by OH^- ions and electrostatic repulsion between negatively charged Fe-HBC surface and anionic arsenate species. In addition to that effect, $HAsO_4^{2-}$ or AsO_4^{3-} which could strengthen the electrostatic repulsion might be dominated in arsenate solution when pH rose above 8. However, the reason of iron-loaded adsorbent being inefficient for As(V) removal at lower pH could be the partial dissolution of iron which makes the adsorbent unstable (Chen et al., 2012). Similarly, a recent study (Repo et al., 2012) reported of iron leaching into the solution at low pH, when the heated lepidocrocite was employed for arsenic removal. Thus, the adsorbent used in this study mainly consisted of iron, aluminum and silicon oxide and could be dissolved at lower pH aqueous solutions. Consequently, the highest iron leaching was recorded (1.2 mg L^{-1}) at pH 2 and decreased when the solution pH increase (Fig. 7).

3.3. Adsorption isotherms

In order to implement a sustainable adsorption system for the adsorption of adsorbate: Langmuir, Freundlich, and Temkin adsorption equations were used to model the sorption equilibrium isotherms and can be expressed in Eqs. (1)–(3), respectively. Adsorption isotherms were obtained at ambient temperature (23 ± 2 °C) and pH 7.5 by varying the initial concentrations of As(V) (100–500 μg L^{-1}). Langmuir model demonstrates a monolayer sorption mechanism with homogeneous sorption energies (Langmuir, 1918; Kundu and Gupta, 2007b), while Freundlich model is an empirical model demonstrating multilayer sorption sites and heterogeneous sorption energies (Freundlich, 1906; Türk et al., 2009). Moreover, Temkin statistical heat of adsorption of all the molecules assumes to be decreased linearly with the surface coverage by adsorbent-adsorbate interaction and hence the binding energies are uniformly distributed (Temkin and Pyzhev, 1940; Kim et al., 2004).

The Langmuir isotherm in its linear form can be expressed as follows: Eq. (1),

$$1/q_e = 1/bQ_0C_e + 1/Q_0 \quad (1)$$

where C_e stands for the concentration of As(V) in μg L^{-1} at equilibrium. The amount of arsenate adsorbed per unit mass of adsorbent q_e(μg g^{-1}), was correlated with the solid-phase concentration at equilibrium. Q_0 and b are Langmuir constants obtained from the slope and intercept of the linear plot $1/q_e$ and $1/C_e$, signifying the amount of metal ions' adsorption corresponding to monolayer coverage and the energy of adsorption, respectively.

The linear form of Freundlich isotherm can be expressed and presents in Eq. (2),

$$\ln q_e = \ln K_f + 1/n \ln C_e \quad (2)$$

where C_e(μg L^{-1}) and q_e(μg g^{-1}) stand for As(V) equilibrium concentrations in liquid and solid phases, respectively. K_f and $1/n$ are the dimensionless constants in the Freundlich isotherm model and related to the relative adsorption capacity (μg g^{-1}) and intensity, respectively.

Moreover, Temkin isotherms model can be expressed as follows: Eq. (3),

$$q_e = RT/b_T \ln A_T + RT/b_T \ln C_e \quad (3)$$

where C_e and q_e as (μg L^{-1}) and (μg g^{-1}) stand for As(V) equilibrium concentrations in liquid and solid phases, respectively. A_T(L μg^{-1}) and b_T(MJ mol^{-1}) are represent Temkin constants. Moreover, here R indicates the universal gas constant 8.314 J mol^{-1} K^{-1} and T is the absolute temperature 303 K. A plot between q_e versus ln C_e determines the isotherm constants A_T and b_T from the slope and the intercept, respectively.

Table 1 Summary of different adsorbents tested to remove As(V) with wide optimum pH ranges.

Adsorbent	Optimum pH	Reference
Sand-red mud column	4–8	Genc-Fuhrman et al. (2005)
Iron-impregnated tablet ceramic adsorbent (ITCA)	4–10	Chen et al. (2012)
Bone char	9–13	Chen et al. (2008)
Iron-coated HBC	6–8	This study

Fig. 8 (a–c) shows the linear plot fittings to Freundlich, Langmuir and Temkin models to sorbed As(V) on Fe-HBC and the evaluated parameters are presented in Fig. 8d. The experimental data showed good isotherm fit and squared correlation coefficients ($R^2 = 0.999$) to linearized Langmuir model. Based on the calculated data in Fig. 8d, it is evident that the linear correlation coefficient (R^2) is in the order of R^2 (Langmuir) > R^2 (Freundlich) > R^2 (Temkin). Therefore, As(V) adsorption isotherm onto Fe-HBC fit to Langmuir model better as compared to Freundlich and Temkin models suggesting monolayer adsorption and indicate adsorbent's surface homogeneity. Moreover, well experimental data fit to both Langmuir and Freundlich isotherm models due to the possibility of both monolayer and heterogeneous energetic distribution of active sites of the respective adsorbents were also discussed (Chiban et al., 2011; Chen et al., 2012). In this study, the sorption capacity of As(V) on Fe-HBC was found to be 961.5 μg g^{-1} in Langmuir isotherm model.

Table 2 presents Langmuir isotherm parameters for As(V) adsorption using Fe-HBC and its comparisons with other adsorbents. The isotherm curve in Langmuir model was considered to predict sorption process in terms of "favorable" and "unfavorable" (Pokhrel and Viraraghavan, 2009). In this regard, Weber and Chakkravorti (1974) defined the important feature in Langmuir isotherm "R_L", a separation factor to describe the adsorption system and can be expressed, as Eq. (4),

$$R_L = 1/1 + K_L C_i \quad (4)$$

where C_i stands for the initial concentration of As(V) (ug L^{-1}), K_L is the Langmuir constant (Eq. (4)). According to R_L value, the following isotherm types could be possible: $R_L > 1$ (unfavorable), $R_L = 1$ (linear), $0 < R_L < 1$ (favorable) and $R_L = 0$ (irreversible). In this study, the value of R_L for the removal of As(V) was calculated to be about 0.118, therefore the isotherm indicated a favorable adsorption.

In the Freundlich model, the value of $1/n$ (intensity of adsorption) more than 1 indicates an unfavorable sorption. In contrast, during favorable sorption in the Freundlich isotherm, the value of $1/n$ falls below 1 (Ranjan et al., 2009) and in this range higher $1/n$ value indicates more affinity and heterogeneity of adsorption sites for efficient adsorption (Mane et al., 2007). However, in this study, $1/n$ value was recorded closer to zero and also clearly evident from R^2 value (0.865) of Freundlich model, as shown in Fig. 8(d). In the Temkin model, the lower linear regression data of R^2 (0.890) showed weaker interaction between adsorbent and adsorbate, and hence did not follow the Temkin isotherm model closely.

3.4. Adsorption kinetic

In this study, the adsorption equilibrium was attained after 14 h using Fe-HBC (Fig. 6). Such a long equilibrium time showed the probability of As(V) diffusion into inner-sphere of the porous adsorbent (Dong et al., 2009). So the comparison of SEM images (Fig. 5a–f) clearly showed that sorption spreads all the pores of each granule and the tabular crystalline grains shaped structure were more obvious (Fig. 5e and f). However, from iron coating the internal pores may not get saturated and efficiently adsorbed As(V).

The linearized form of Pseudo-second order (PSO) kinetic model can be expressed (Ho and Mckay, 2000), as follows: Eq. (5),

$$t/q_t = 1/(k_2 q_e^2) + t/q_e t \quad (5)$$

where q_e and q_t are the amount of As(V) adsorbed (mg g^{-1}) by the adsorbent at the equilibrium time and at time t (min), respectively. In Eq. (5), k_2 is the pseudo-second order sorption rate constant (g mg^{-1} min^{-1}). Table 3 presents the calculated value of different correlation coefficients observed with different adsorbent doses (0.01–0.05 g). It showed that the

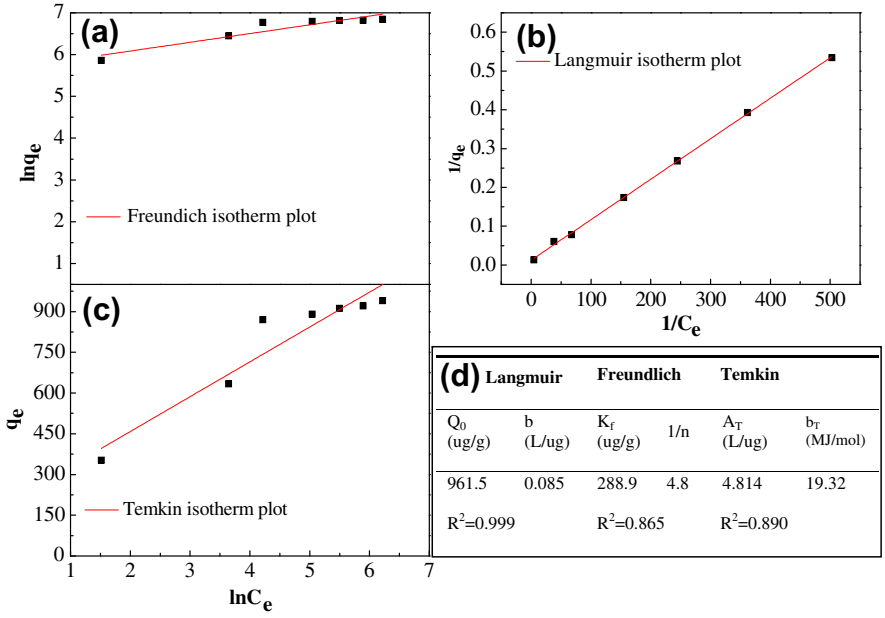

(d)

Langmuir		Freundlich		Temkin	
Q_0 (ug/g)	b (L/ug)	K_f (ug/g)	1/n	A_T (L/ug)	b_T (MJ/mol)
961.5	0.085	288.9	4.8	4.814	19.32
R^2=0.999		R^2=0.865		R^2=0.890	

Figure 8 Isotherm plots for As(V) adsorption in the following reaction conditions: adsorbent dose = 0.04 g/150 mL, solution pH = 7.5, pH, equilibrium time = 14 h, temperature = 23 ± 2 °C. Moreover, (a) present Freundlich isotherm plot, (b) Langmuir isotherm plot, (c) Temkin isotherm plot and (d) present the values As(V) adsorption isotherm parameters derived from Langmuir, Freundlich and Temkin model equations.

Table 2 Langmuir isotherm parameters of As(V) adsorption using iron-coated HBC and comparison with other adsorbents.

Adsorbent	pH	Duration (h)	Temperature (°C)	Initial conc. (mg/L)	Capacity (mg/g)	Reference
Iron-coated pottery granules (ICPG)	7.0	24	25	0.13	1.74	Dong et al. (2009)
Iron-impregnated tablet ceramic adsorbent (TCA)	6.9	48	25	5–100	8.49	Chen et al. (2012)
Bone char	10	1	28 ± 2	0.5–1.5	1.43	Chen et al. (2008)
Rice polish	4	2.5	20	0.1–1.0	0.147	Ranjan et al. (2009)
Magnetic wheat straw (MWS)	7.0	12	30	1–28	8.02	Tian et al. (2011)
Iron-coated HBC	7.5	14	23 ± 2	0.1–0.5	0.961	This study

PSO was the divine pathway for the reaction to achieve equilibrium.

3.5. Effect of competing ions

Due to the complexity of dissolved substances in natural water, there might be competition from other species including Cl^-, F^-, HCO_3^-, and PO_4^{3-} which may largely deteriorate the arsenic removal performance by competing with arsenic for active sorption sites (Suzuki et al., 2000; Ntim and Mitra, 2012). In this study, the effects of Cl^-, F^-, HCO_3^- and PO_4^{3-} on the removal of As(V) over the concentration ranges (0.1–10 mM) were investigated. Fig. 9 presents As(V) removal result in the presence of various anions. It revealed that the presence of Cl^- and F^- had almost negligible effect of As(V) adsorption on Fe-HBC which is inconsistent with the recently reported studies (Ntim and Mitra, 2012; Tanboonchuy et al., 2012). In the presence HCO_3^- at a concentration range of 10 mM has slightly inhibited As(V) removal (Fig. 9). The reasons could be the competition between HCO_3^- and As(V) species for the adsorptive sites on Fe-HBC to form complexes with iron (oxy)hydroxides (Dong et al., 2009; WHO, 2011). Additionally, iron (oxy)hydroxides formed from Fe(II) oxidation hence generated several favorable sites for As(V) adsorption (Tanboonchuy et al., 2012). In this study, the interference of the competing anions on an mM basis follows: $PO_4^{3-} > HCO_3^- > F^- > Cl^-$.

The presence of PO_4^{3-} even at low concentration (0.1 mM) inhibited the removal performance of As(V). It may be attributed to their similar geochemical behaviors and surface chemistry, and both anions compete for the adsorption sites (Tanboonchuy et al., 2012). Furthermore, PO_4^{3-} adsorbed on iron(oxy) hydroxides to form inner-sphere surface complexes with OH^- group (Hsu et al., 2008). Recently, Meng and co-workers (Meng et al., 2002) had reported that the affinity of PO_4^{3-} to iron(oxy) hydroxides was stronger than the arsenic species. Additionally, its high inhibiting effect to remove As(V) at elevated pH value was also confirmed from a previously reported study (Su and Puls, 2001) which indicated that at high pH, less positively surface charged sites was available on the adsorbent's surface. Nonetheless, experimental result demonstrated that the binding attractions of Cl^- and F^- for Fe-HBC were weaker, but HCO_3^- and PO_4^{3-} were comparable to that of As(V).

Table 3 Pseudo-second-order rate constants for As(V) adsorption at the studied adsorbent dose.

Adsorbent dose (g/150 mL)	q_e (mg/g)	K_2 (g/(mg min))	R^2
0.01	0.515	58.77	0.976
0.02	0.495	33.77	0.944
0.03	0.437	36.59	0.971
0.04	0.379	40.13	0.994
0.05	0.300	91.16	0.980

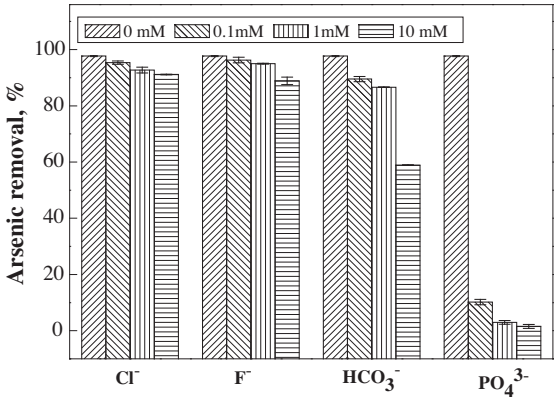

Figure 9 Effect of various competing ions on As(V) removal by Fe-HBC. Reaction condition: initial As(V) = 100 ppb, solution pH = 7.5, adsorbent dose = 0.04 g/150 mL, contact time = 14 h.

3.6. Classification of the exhausted adsorbent

The life-cycle assessment of any adsorbent material is critically important to assess its ecological and environmental impacts. The adsorbent (HBC) used in the present study was waste and available for free, as recently evaluated by Yue et al. (2011). For this purpose, Toxicity characteristic leaching procedure (TCLP) was employed to assess the exhausted media as hazardous or immobile waste. Non-detectable (ND) result of arsenic from the spent adsorbents revealed that the media is non-hazardous and can be safely used in municipal applications. Moreover, it also suggests that the adsorbed arsenic may either be tightly bound with the surface's charge of the adsorbent or formed the structural components of fresh

(oxy)hydroxide minerals (Guo et al., 2007). It indicates that the life-cycle assessment of HBC as adsorbent is considered to be environmentally friendly and sustainable.

4. Conclusions

Iron-coated HBC was successively developed from the locally generated wastes for the adsorptive removal of As(V) from aqueous solutions. The silent feature of the prepared adsorbent is its granular surface, high sorption capacity for As(V), massive local availability and least waste generation. Detailed characterizations revealed that the Fe-HBC has less surface complexity, more surface area and observed better performance to remove As(V) at pH range (6–8) with the adsorption capacity of 961.5 μg g^{-1}. The experimental data of equilibrium adsorption isotherms fit the Langmuir model the best and confirmed adsorbent's surface homogeneity and monolayer adsorption. With acidification (pH < 4) quite highly dissolved iron leaching (1.2 mg L^{-1}) into the solution showed less As(V) binding and that resulted in lower As(V) removal. Competing ions especially PO_4^{3-} even at low concentration (0.1 mM) inhibited As(V) removal and that could be the stronger affinity of PO_4^{3-} to iron(oxy) hydroxides than arsenic species. Non-detectable result of arsenic in the spent media showed non-hazardous properties of the material and could be used in different fields. The use of HBC as sorbent material for pollutant remediation is highly promising due to its sustainable production, high uptake capacity and local availability in scattered settlements.

Acknowledgements

The authors would like to thank the National Natural Science Foundation (No. 21277119) and the Science and Technology Project of Zhejiang Province, China (No. 2012C23061) for the financial supports. S.A. Baig acknowledges Chinese Scholarship Council (CSC) of the People's Republic of China for a PhD scholarship.

References

Baig, S.A., Sheng, T., Hu, Y., Xu, J., Xu, X., 2013. Arsenic removal from natural water using low cost granulated adsorbents: a review. Clean-Soil Air Water. http://dx.doi.org/10.1002/clen.201200466.

Barakat, M.A., Shah, S.I., 2013. Utilization of anion exchange resin Spectra/Gel for separation of arsenic from water. Arabian J. Chem 6, 307–311.

Bodek, I., Lyman, W.J., Reehl, W.F., Rosenblatt, D.H., 1998. Environmental Inorganic Chemistry: Properties Processes and Estimation Methods. Pergamon Press, USA.

Chen, Y., Chai, L., Shu, Y., 2008. Study of arsenic(V) adsorption on bone char from aqueous solution. J. Hazard. Mater. 160, 168–172.

Chen, R.Z., Zhang, Z.Y., Lei, Z.F., Sugiura, N., 2012. Preparation of iron-impregnated tablet ceramic adsorbent for arsenate removal from aqueous solutions. Desalination 286, 56–62.

Chiban, M., Carja, G., Lehutu, G., Sinan, F., 2011. Equilibrium and thermodynamic studies for the removal of As(V) ions from aqueous solution using dried plants as adsorbents. Arabian J. Chem.. http://dx.doi.org/10.1016/j.arabjc.2011.10.002.

Dong, L.J., Zinin, P., Cowen, J., Ming, L., 2009. Iron coated pottery granules for arsenic removal from drinking water. J. Hazard. Mater. 168, 626–632.

Fan, Y., Zhang, F., Feng, Y., 2008. An effective adsorbent developed from municipal solid waste and coal co-combustion ash for As(V) removal from aqueous solution. J. Hazard. Mater. 159, 313–318.

Feng, L.Y., Cao, M.H., Ma, X.Y., Zhu, Y.S., Hu, C.W., 2012. Superparamagnetic high-surface-area Fe_3O_4 nanoparticles as adsorbents for arsenic removal. J. Hazard. Mater. 217–218, 439–446.

Francesca, G., Giancarla, A., Nuria, Fiol, Isabel, V., 2013. Application of anodic stripping voltammetry to assess sorption performance of an industrial waste entrapped in alginate beads to remove As(V). Arabian J. Chem. (http://dx.doi.org/10.1016/j.arabjc.2013.01.003).

Freundlich, H., 1906. Concerning adsorption in solutions. Zeitschrift Fur Physikalische Chemie-Stochiometrie Verwandtschaftslehre 57, 385–470.

Genc-Fuhrman, H., Tjell, J.C., McConchie, D., 2004a. Adsorption of arsenic from water using activated neutralized red mud. Environ. Sci. Technol. 38 (8), 2428–2434.

Genc-Fuhrman, H., Tjell, J.C., McConchie, D., 2004b. Increasing the arsenate adsorption capacity of neutralized red mud (Bauxsol). J. Colloid Interface Sci. 271, 313–320.

Genc-Fuhrman, H., Bregnhoj, H., McConchie, D., 2005. Arsenate removal from water using sand red mud columns. Water Res. 39, 2944–2954.

Gu, Z., Fang, J., Deng, B., 2005. Preparation and evaluation of GAC-based iron containing adsorbents for arsenic removal. Environ. Sci. Technol. 39, 3833–3843.

Guo, H.M., Stuben, D., Berner, Z., 2007. Arsenic removal from water using natural iron mineral-quartz sand columns. Sci. Total Environ. 377, 142–151.

Ho, Y.S., Mckay, G., 2000. The kinetics of sorption of divalent metal ions onto sphagnum moss peat. Water Res. 34 (3), 735–742.

Hristovski, K.D., Westerhoff, P.K., Moller, T., Sylvester, P., 2009. Effect of synthesis conditions on nano-iron (hydro) oxide impregnated granulated activated carbon. Chem. Eng. J. 146, 237–243.

Hsu, J.C., Lin, C.J., Liao, C.H., Chen, S.T., 2008. Evaluation of the multiple-ion competition in the adsorption of As(V) onto reclaimed iron-oxide coated sands by fractional factorial design. Chemosphere 72, 1049–1055.

Jing, C.Y., Cui, J., Huang, Y.Y., Li, A.G., 2012. Fabrication, characterization, and application of a composite adsorbent for simultaneous removal of arsenic and fluoride. Appl. Mater. Interfaces 4, 714–720.

Kim, Y., Kim, C., Choi, I., Rengraj, S., Yi, J., 2004. Arsenic removal using mesoporous alumina prepared via a templating method. Environ. Sci. Technol. 38, 924–931.

Kundu, S., Gupta, A.K., 2006. Arsenic adsorption onto iron oxide-coated cement (IOCC): regression analysis of equilibrium data with several isotherm models and their optimization. Chem. Eng. J. 122, 93–106.

Kundu, S., Gupta, A.K., 2007a. As(III) removal from aqueous medium in fixed bed using iron oxide-coated cement (IOCC): experimental and modeling studies. Chem. Eng. J. 129, 123–131.

Kundu, S., Gupta, A.K., 2007b. Adsorption characteristics of As(III) from aqueous solution on iron oxide coated cement (IOCC). J. Hazard. Mater. 142, 97–104.

Lakshmipathiraj, P., Narasimhan, B.R.V., Prabhakar, S., Bhaskar Raju, G., 2006. Adsorption of arsenate on synthetic goethite from aqueous solutions. J. Hazard. Mater. 136 (2), 281–287.

Langmuir, I., 1918. The adsorption of gases on plane surfaces of glass, mica and platinum. J. Am. Chem. Soc. 40, 1361–1403.

Li, Y.R., Wang, J., Luan, Z.K., Liang, Z., 2010. Arsenic removal from aqueous solution using ferrous based red mud sludge. J. Hazard. Mater. 177, 131–137.

Maji, S.K., Kao, Y., Wang, C., Lu, G., Wu, J., Liu, C., 2012. Fixed bed adsorption of As(III) on iron-oxide-coated natural rock (IOCNR) and application to real arsenic-bearing groundwater. Chem. Eng. J. 203, 285–293.

Malik, A.H., Khan, Z.M., Mahmood, Q., Nasreen, S., Bhatti, Z.A., 2009. Prospective of low cost arsenic remediation in Pakistan and other developing countries. J. Hazard. Mater. 168, 1–12.

Mandal, B.K., Suzuki, K.T., 2002. Arsenic around the world: a review. Talanta 58, 201–235.

Mane, V.S., Mall, I.D., Srivastava, V.C., 2007. Kinetic and equilibrium isotherm studies for the adsorptive removal of Brilliant Green dye from aqueous solution by rice husk ash. J. Environ. Manag. 84, 390–400.

Mathieu, J.L., Gadgil, A.J., Addy, S.E.A., Kowolik, K., 2010. Arsenic remediation of drinking water using iron-oxide coated coal bottom ash. J. Environ. Sci. Health Part A 45, 1446–1460.

Meng, X.G., Korfiatis, G.P., Bang, S., Bang, K.W., 2002. Combined effects of anions on arsenic removal by iron hydroxides. Toxicol. Lett. 133, 103–111.

Mikhaylova, Y., Adam, G., Huassler, L., Eihhorn, K.-J., Voit, B., 2006. Temperature-dependent FTIR spectroscopic and thermoanalytic studies of hydrogen bonding of hydroxyl (phenolic group) terminated hyper branched aromatic polyesters. Mol. Struct. 788 (1–3), 80–88.

Mohan, D., Pittman, C.U., 2007. Arsenic removal from water/wastewater using adsorbents-a critical review. J. Hazard. Mater. 142, 1–53.

Mohan, D., Pittman Jr., C.U., Bricka, M., Smith, F., Yancey, B., Mohammad, J., Steele, P.H., Alexandre-Franco, M.F., Serrano, V.G., Gong, H., 2007. Sorption of arsenic, cadmium, and lead by chars produced from fast pyrolysis of wood and bark during bio-oil production. J. Colloid Interface Sci. 310 (1), 57–73.

Mondal, P., Majumder, C.B., Mohanty, B., 2008. Effects of adsorbent dose, its particle size and initial arsenic concentration on the removal of arsenic, iron and manganese from simulated ground water by Fe^{3+} impregnated activated carbon. J. Hazard. Mater. 150, 695–702.

Ntim, S.A., Mitra, S., 2012. Adsorption of arsenic on multiwall carbon nanotube-zirconia nanohybrid for potential drinking water purification. J. Colloid Interface Sci. 375, 154–159.

Pokhrel, D., Viraraghavan, T., 2009. Biological filtration for removal of arsenic from drinking water. J. Environ. Manage. 90, 1956–1961.

Ranjan, D., Talat, M., Hasan, S.H., 2009. Biosorption of arsenic from aqueous solution using agricultural residue 'rice polish'. J. Hazard. Mater. 166, 1050–1059.

Repo, E., Mäkinen, M., Rengaraj, S., Natarajan, G., Bhatnagar, A., Sillanpää, M., 2012. Lepidocrocite and its heat-treated forms as effective arsenic adsorbents in aqueous medium. Chem. Eng. J. 180, 159–169.

Roberts, L.C., Hug, S.J., Ruettimann, T., Billah, M.M., Khan, A.W., Rahman, M.T., 2004. Arsenic removal with iron(II) and iron(III) in waters with high silicate and phosphate concentrations. Environ. Sci. Technol. 38, 307–315.

Sarkar, S., Gupt, A., Biswas, R.K., Deb, A.K., Greenleaf, J.E., Sen-Gupta, A.K., 2005. Well-head/arsenic removal units in remote villages of Indian subcontinent: Field results and performance evaluation. Water Res. 39, 2196–2206.

Su, C.M., Puls, R.W., 2001. Arsenate and arsenite removal by zerovalent iron: effect of phosphate, silicate, carbonate, borate, sulfate, chromate, molybdate, and nitrate, relative to chloride. Environ. Sci. Technol. 35, 4562–4568.

Suzuki, T.M., Bomani, J.O., Matsunaga, H., Yokoyama, T., 2000. Preparation of porous resin loaded with crystalline hydrous zirconium oxide and its application to the removal of arsenic. React. Funct. Polym. 43, 165–172.

Tanboonchuy, V., Grisdanurak, N., Liao, C.H., 2012. Background species effect on aqueous arsenic removal by nano zero-valent iron using fractional factorial design. J. Hazard. Mater. 205–206, 40–46.

Temkin, M., Pyzhev, V., 1940. Kinetics of ammonia synthesis on promoted iron catalysts. Acta Physicochim. Urss 12, 327–356.

Tian, Y., Wu, M., Lin, X.B., Huang, P., Huang, Y., 2011. Synthesis of magnetic wheat straw for arsenic adsorption. J. Hazard. Mater. 193, 10–16.

Türk, T., Alp, I., Deveci, H., 2009. Adsorption of As(V) from water using Mg-Fe-based hydrotalcite (FeHT). J. Hazard. Mater. 171, 665–670.

USEPA, 2000. Arsenic Treatment Technology Evaluation Handbook for Small System. EPA 816-R-03-014. USEPA, Washington, DC.

Weber, T.W., Chakkravorti, R.K., 1974. Pore and solid diffusion models for fixed bed adsorbers. Am. Institute Chem. Eng. J. 20, 228–232.

WHO, 2011. Guidelines for Drinking Water Quality, fourth ed. World Health Organization, Geneva, Switzerland.

Xu, J., Tang, J., Baig, S.A., Lv, X., Xu, X., 2013. Enhanced dechlorination of 2,4-dichlorophenol by Pd/Fe-Fe_3O_4, nanocomposites. J. Hazard. Mater. 244–245, 628–636.

Yue, X., Li, X.M., Wang, D.B., Shen, T.T., Liu, X., Yang, Q., Zeng, G.M., Liao, D.X., 2011. Simultaneous phosphate and COD_{cr} removals for landfill leachate using modified honeycomb cinders as an adsorbent. J. Hazard. Mater. 190, 553–558.

Zhu, K., Sun, C., Chen, H., Baig, S.A., Sheng, T., Xu, X., 2013. Enhanced catalytic hydrodechlorination of 2,4-dichlorophenoxyacetic acid by nanoscale zerovalent iron with electrochemical technique using a palladium/nickel foam electrode. Chem. Eng. J. 223, 192–199.